Development of spin-orbit coupling for stochastic configuration interaction techniques

Development of Spin-Orbit Coupling for Stochastic Configuration Interaction Techniques

Paul Murphy, Jeremy P. Coe, and Martin J. Paterson*

October 30, 2017

Abstract

In order to perform spin-orbit coupling calculations on atoms and molecules, good zeroth-order wavefunctions are necessary. Here, we present the software development of the Monte Carlo Configuration Interaction (MCCI) method, to enable calculation of such properties, where MCCI iteratively constructs a multi-reference wavefunction using a stochastic procedure. In this initial work, we aim to establish the efficacy of this technique in predicting the splitting of otherwise degenerate energy levels on a range of atoms and small diatomic molecules. It is hoped that this work will subsequently act as a gateway towards using this method to investigate singlet-triplet interactions in larger multi-reference molecules. We show that MCCI can generate very good results using highly compact wavefunctions compared to other techniques, with no prior knowledge of important orbitals. Higher-order relativistic effects are neglected and spin-orbit coupling effects are incorporated using first-order degenerate perturbation theory with the Breit-Pauli Hamiltonian and effective nuclear charges in the one-electron operator. Results are obtained and presented for B, C, O, F, Si, S and Cl atoms and OH, CN, NO and C_2 diatomic radicals including spin-orbit coupling constants and the relative splitting of the lowest energy degenerate state for each species. Convergence of MCCI to the full configuration interaction (FCI) result is demonstrated on the multireference problem of stretched OH. We also present results from the singlet-triplet interaction between the $X^3\Sigma_g^-$ and both the $a^1\Delta_g$ and $b^1\Sigma_g^+$ states of the O_2 molecule.

Keywords: spin-orbit coupling, Breit-Pauli Hamiltonian, O_2 molecule, Monte Carlo Configuration Interaction, stochastic.

*Institute of Chemical Sciences, School of Engineering and Physical Sciences, Heriot-Watt University, Edinburgh, EH14 4AS, UK, (m.j.paterson@hw.ac.uk)

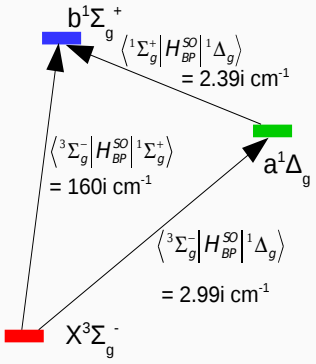

We have developed the stochastic method Monte Carlo Configuration Interaction to calculate spin-orbit coupling properties of a range of atoms and molecules using the Breit-Pauli Spin-Orbit Hamiltonian with effective nuclear charges in the one-electron operator. Following the initial proof-of-concept, we present successful predictions of spin-orbit matrix elements between the $X^3\Sigma_g^-$, $\mathrm{a}^1\Delta_g$ and $b^1\Sigma_g^+$ states of molecular oxygen in order to demonstrate general applicability of the technique using highly compact wavefunctions with no prior knowledge or assumption of the important orbitals.

INTRODUCTION

Spin-orbit coupling effects play a vital role in a range of phenomena from the removal of degeneracy of energy levels to phosphorescence in living animals through inter-system crossings. When electronic excited states are close in energy to the ground state, spin-orbit coupling can allow non-spin conserving chemical reactions and processes to proceed through these excited states when normally, such reactions would be forbidden by selection rules.[1] Examples include mixing of singlet-triplet states of the trimethylene biradical[2], inter-system crossing in conjugated polymers[3] and finally the elucidation of potential energy surfaces, spectroscopic constants, avoided crossings and radiative lifetimes of triplet states for halogen diatomic molecules.[4,5,6]

Exact calculations of spin-orbit effects involves solving the fully relativistic Dirac equation. This proves cumbersome computationally and efforts to find solutions to this problem have traditionally relied on the Breit-Pauli Spin-Orbit Hamiltonian. This Hamiltonian approximates relativistic effects whilst neglecting higher-order effects and is shown in equation 1 with the individual terms described in equations 2, 3 and 4 where $\mathcal{H}_{ne}^{so}$ is the interaction between the electron spin and the orbital angular momentum as the electron moves around the nucleus, $\mathcal{H}_{ee}^{so}$ is the interaction between electron spin and the angular momentum caused by the electron moving around other electrons and $\mathcal{H}_{ee}^{soo}$ is the interaction between the electron spin and the angular momentum of other electrons moving around it. $\hat{s}(i)$ is the spin angular momentum operator for electron i, $\hat{p}_i$ is the linear momentum operator for electron i, N_{elec} is the number of electrons, N_{nuc} is the number of nuclei, r_{ij} is the distance between electrons i and j, r_{iA} is the distance between electron i and nucleus A, Z_A is the charge of nucleus A and c is the speed of light.

$$\mathcal{H}_{BP}^{so} = \mathcal{H}_{ne}^{so} + \mathcal{H}_{ee}^{so} + \mathcal{H}_{ee}^{soo} \tag{1}$$

$$\mathcal{H}_{ne}^{so} = \frac{1}{2c^2} \sum_{i=1}^{N_{elec}} \sum_{A=1}^{N_{nuc}} Z_A \frac{\hat{s}(i) \cdot (\hat{r}_{iA} \times \hat{p}_i)}{r_{iA}^3} \tag{2}$$

$$\mathcal{H}_{ee}^{so} = -\frac{1}{2c^2}\sum_{i=1}^{N_{elec}}\sum_{j\neq i}^{N_{elec}}\frac{\hat{s}(i)\cdot(\hat{r}_{ij}\times\hat{p}_i)}{r_{ij}^3} \tag{3}$$

$$\mathcal{H}_{ee}^{soo} = -\frac{1}{c^2}\sum_{i=1}^{N_{elec}}\sum_{j\neq i}^{N_{elec}}\frac{\hat{s}(i)\cdot(\hat{r}_{ij}\times\hat{p}_j)}{r_{ij}^3} \tag{4}$$

This paper describes a new method for calculating spin-orbit properties and we demonstrate the concept on a range of atoms and diatomic molecules. We therefore present a brief, non-exhaustive, background on some of the pertinent literature in this regard.

Blume *et al.*[7,8] evaluated the Breit-Pauli Hamiltonian for a range of atoms, discovering that interactions between unpaired valence electrons and core electrons provided an effective one-electron spin-orbit interaction and this was considered to provide effective shielding of the valence electrons from the nuclear framework resulting in a reduction of the spin orbit coupling constant. Using a Hartree-Fock wavefunction, results for the spin-orbit coupling constant were found to have around 6.11% error compared to experiment for a selection of first and second row atoms.

Walker *et al.*[9] followed this work by considering the effect of spin-orbit coupling on the hydrides of elements in the first row of the periodic table and also on small diatomics such as BO and CO. For first row hydrides, the neglect of two-electron terms was less important than for diatomics where the mass was more equally balanced between the atoms, such as with CO. The spin-orbit coupling constant for OH was found to be -141.40 cm^{-1} compared to -139.21 cm^{-1} found experimentally.

Using CASSCF as the zeroth order wavefunction for investigating diatomic molecules along with the use of effective nuclear charges, Koseki *et al.*[10] found that results on first row hydrides were within 10 cm^{-1} of experiment for the spin-orbit coupling constants. For more general diatomics such as NO, OH and CN, spin-orbit coupling constants were found to be within 6 cm^{-1} of experiment.

The use of CI as a zeroth order wavefunction for spin-orbit coupling calculations was investigated by Heß *et al.*[11] with multi-centre two-electron spin-orbit terms excluded. One centre two-electron terms were then constructed in the average field of the remaining electrons which appeared in at least one configuration. This technique was then applied to palladium

complexes such as PdCl and Pd_2^+ resulting in errors in the spin-orbit coupling constant of just 2 cm^{-1} compared to experiment.

In a further attempt to simplify the two-electron spin-orbit integrals, Nicklass *et al.*[12] used MRCI to investigate the role of the basis set in spin-orbit calculations of the splitting of degenerate ground states of atoms such as F, Cl and Br. It was found that the inclusion of *2p* functions had a large impact on F although this was found to be less so for Cl and Br. Inclusion of higher angular momentum functions, diffuse functions and increasing the active space to include more virtual orbitals was found to have a negligible effect. Correlation of core electrons was found to be considerably more important than correlation of valence electrons. This work was extended by Berning *et al.*[13] who used an effective one-electron spin-orbit operator. Only the most important two-electron integrals were used in order to capture core effects as completely as possible with virtually no loss in accuracy. It was found that two-electron terms are more important for smaller atoms, becoming less important for larger atoms. The neglect of two-electron integrals involving valence electrons resulted in errors less than 1%.

More recently, Tu *et al.*[14] have used equation of motion coupled cluster techniques alongside inclusion of spin-orbit coupling effects to determine a range of states of ionised atoms up to the 5th row (EOM-IP-CC). Ionisation potentials were found to be in reasonable agreement with experiment when spin-orbit effects were included and acceptable spin-orbit splitting values were also observed. Although both CCS and CCSD methods were attempted, problems were highlighted when using CCS on the I_2^+ ion where the stable $^2\Sigma_g^+$ state was incorrectly predicted to be unbound.

Epifanovsky *et al.*[15] investigated the performance of a range of EOM-CCSD variants including those developed for excitation energies (EOM-EE-CCSD), spin-flip (EOM-SF-CCSD), ionisation potential (EOM-IP-CCSD) and electron attachment (EOM-EA-CCSD). Spin-orbit effects were introduced using the Breit-Pauli Hamiltonian and a perturbative approach. All variants were found to perform well although some problems were encountered in biradical systems where the choice of variant was crucial to obtaining accurate results. Spin-orbit splitting values of degenerate states of a range of atoms and small molecules including C, O, S, Si, NO and OH exhibited errors less than 5% compared to experiment.

Mück *et al*[16], created a general multi-reference coupled cluster scheme (MRCC) using an effective mean-field spin-orbit operator for open-shell systems. A range of diatomic and triatomic molecules were considered including species such as OH, SH, ClO, CCF and NCS. Results of spin-orbit splittings were shown to be in good agreement with experiment.

In search of a black box technique, density-functional theory (DFT) was investigated as a foundation for spin-orbit calculations by Roemelt *et al.*[17]. This method was based on restricted open-shell single excitations (DFT/ROCIS) using a mean field approximation of the Breit-Pauli equation for spin-orbit effects. Dynamic correlation was accounted for in an averaged manner using empirical parameterisation. L-edge X-ray absorption of various transition metal complexes involving Cu, Ti, Fe and Ni showed near quantitative results in some circumstances when spin-orbit coupling effects were taken into account. Other work by Maganas *et al.*[19], using this technique, involved elucidation of the near edge X-ray absorption fine structure (NEXAFS) of V_2O_5, finding excellent agreement with experiment. It is their intention that this technique applied to NEXAFS could be used in the future to better understand catalytic reactions.

On the macroscale, Irmer *et al.*[18] undertook a first principles investigation of the spin-orbit coupling within fluorinated graphene using DFT. Very large spin-orbit coupling effects were detected in contrast to hydrogenated graphene. It was concluded that these effects were as a result of the interaction between the fluorine atoms and the carbon atoms rather than through σ-π hybridisation due to structural deformation as found with hydrogenised graphene. This work is expected to be used in future studies involving quantum transport simulations which display spin-orbit coupling effects and other applications which involve physical phenomena close to the Fermi level of fluorinated graphene.

Coupled cluster (SOCC) and configuration interaction (SOCI) methods were used alongside relativistic effective core potentials (RECP) by Kim *et al.*[20] to investigate spin-orbit effects in a range of heavy atom hydrides such as TlH, BiH, PbH, PoH and AtH. It was demonstrated that the SOCC method displayed relative invariance to the strength of the spin-orbit coupling effects and very good results were obtained relative to FCI when measuring both absolute energies and equilibrium bond lengths. It was however conceded that such a method will only be effective on systems which can be described as largely single reference.

Spectroscopic properties of a range of small molecules which are best described by multi-reference methods, can be determined by traditional MRCI methods using the Breit-Pauli Hamiltonian. One such molecule, AsN, was investigated by Liu *et al.*[21]. The potential energy surfaces of a wide range of electronic states were obtained for the molecule with excellent results observed in comparison to available experimental measurements.

Finally, we mention the work of Chiodo *et al.*[22,23,24] who approximated the two-electron terms of the Breit-Pauli Hamiltonian by introducing an effective nuclear charge Z_{eff} into the one-electron term via a scaling term λ. These scaling factors were deduced through fitting to Fine Structure Splitting (FSS) calculations for doublet and triplet Π states for AH hydrides using the full Breit-Pauli Hamiltonian, where A is any element up to and including the fifth row of the periodic table. A range of diatomic molecules were tested, showing excellent agreement between DFT results obtained via the effective one-electron terms and those obtained using the full Breit-Pauli Hamiltonian.

In this paper, Monte Carlo Configuration Interaction (MCCI)[25,26,27,28] is used to provide an improved zeroth order wavefunction prior to the calculation of spin-orbit effects. The objective of MCCI is to describe a correlated system using a highly compact wavefunction with no prior knowledge or assumptions about the important orbitals. In doing so, it approximates the Full Configuration Interaction (FCI) solution of the system. This is achieved by iteratively constructing a wavefunction using random single and doubly excited electron configurations at every step. A restricted or unrestricted Hartree-Fock wavefunction is normally used as the initial reference[29] (with integrals available from supported quantum chemical packages such as Molpro[30] and Columbus[31]) and it is worth noting that, in principle, any number of excitations in a determinant may eventually be reached as the calculation progresses. This *branching* stage terminates after a programmable number of configurations have been added to the wavefunction. Following the *branching* stage, the Hamiltonian matrix is constructed in the basis of electronic configurations and *diagonalised* to produce a set of coefficients for each configuration. A *pruning* step removes all configurations from the wavefunction which have values below a certain programmable cutoff threshold, c_{min}. Convergence is then achieved when the change in energy after each *branching/diagonalisation/pruning* cycle falls within the convergence criteria. In this way, MCCI

is capable of capturing a large portion of static correlation using only a very small fraction of the Full Configuration Interaction space. It is also capable of capturing some dynamic correlation and contains support for a second-order perturbative treatment of the wavefunction.[32]

MCCI has been used in several applications. Győrffy *et al.*[33] applied the technique to calculate a few singlet and triplet excitation energies of a small number of molecules such as CH_2 and H_2O. Remarkable results were obtained which came within a few tenths of eV compared to the FCI solution with just a few thousand configurations as opposed to the hundreds of millions required by FCI. These results were essentially identical to those achieved using EOM-CCSDT. Ground state potential energies were explored by Coe *et al.*[34] who investigated dissociation of small molecules such as N_2, F_2, HF, CH_4 and the H_{50} lattice. Results for the dimers were found to approach FCI results, again at a fraction of the FCI space. Ground state potential energy surfaces for systems such as NH_3 inversion and ethylene torsion were also considered with results approaching chemical accuracy in some cases. Following this ground state potential energy work, Coe *et al.*[35] found MCCI useful in finding accurate multipole moments for a variety of molecules such as NO (dipole), N_2 (quadrupole) and CH_4 (octupole) in addition to ionisation potentials for the first row atoms, together with Na and Mg, which had at most 1.2% error compared to FCIQMC[36] results. Electron affinities were found to be less accurate though, probably as a result of the small magnitude of these quantities relative to the stochastic noise inherent in a random technique such as MCCI. A form of state averaging was also implemented[37] in order to calculate excited states without root-flipping problems. Excellent results were obtained for the H_3 molecule. Finally, other applications of MCCI include calculations of higher-order dipole properties[38], Xray emission and absorption energies[39], positronic systems[40] and the potential energy surfaces of transition metal dimers.[41]

Our intention, in this paper, is to demonstrate that a balance can be struck between obtaining sufficiently accurate spin-orbit coupling properties and using highly compact wavefunctions with relatively small basis sets and the one-electron part of the Breit-Pauli Hamiltonian (using effective nuclear charges to compensate for neglect of the two-electron terms). It is hoped that this proof of concept work can open the door to potential application of the

technique to larger multi-reference molecules. Crucially, we seek to demonstrate that this can be achieved with no prior knowledge of, or assumptions about, the important orbitals of the system.

METHODOLOGY

We consider chemical systems where spin-orbit interactions are extremely small with respect to the difference in energy between electronic states. For systems involving only atoms from the first three rows of the periodic table, use of the Breit-Pauli Hamiltonian is justified and high-order effects can be neglected. Spin-orbit interactions are then implemented using first-order degenerate perturbation theory. The $\mathcal{H}_{ee}^{so}$ and $\mathcal{H}_{ee}^{soo}$ terms of equation 1 are approximated using an effective nuclear charge[22,23,24] Z_{eff}, in place of the bare nuclear charge, Z_A in the one-electron $\mathcal{H}_{ne}^{so}$ term. This is shown in equation 5 where $Z_{eff}(A)$ is the effective nuclear charge for atom A, λ_A is a scaling factor for atom A and Z_A is the bare nuclear charge of atom A. The value of λ_A is atom specific and is described in literature[22,23,24]. As discussed earlier, these scaling factors are deduced through fitting to Fine Structure Splitting (FSS) calculations for doublet and triplet Π states for AH hydrides using the full Breit-Pauli Hamiltonian. For convenience, we reproduce these literature values in equation 6, for atoms B to F, and equation 7, for atoms Al to Cl. In these latter two equations, N^{val} is the number of valence electrons for atom A. We therefore use the effective one-electron Hamiltonian shown in equation 8 where the individual variables are described earlier in the discussion of equation 2.

$$Z_{eff}(A) = \lambda_A Z_A \tag{5}$$

$$\lambda_A(B-F) = 0.2517 + 0.0626N^{val} \tag{6}$$

$$\lambda_A(Al-Cl) = 0.7213 + 0.0144N^{val} \tag{7}$$

$$\mathcal{H}^{so} = \frac{1}{2c^2} \sum_{i=1}^{N_{elec}} \sum_{A=1}^{N_{nuc}} Z_{eff}(A) \frac{\hat{s}(i) \cdot (\hat{r}_{iA} \times \hat{p}_i)}{r_{iA}^3} \tag{8}$$

Our test-bank for this work consists of the following atoms and molecules with states shown in parentheses: B(^{2}P), C(^{3}P), O(^{3}P), F(^{2}P), Si(^{3}P), S(^{3}P), Cl(^{2}P), OH($X^2\Pi$), CN($A^2\Pi$), C_2($a^3\Pi_u$) and NO($X^2\Pi$). These states are the lowest for which degeneracy exists for each species. Mixing of higher energy states is neglected throughout, although as the states above are fairly well isolated energetically, this should not cause undue errors in the calculations. The bond lengths for the diatomic molecules are as follows: CN (1.2333 Å), OH (0.96966 Å), NO (1.15077 Å) and C_2 (1.3119 Å). For absolute energy and spin-orbit matrix element convergence with basis set and c_{min}, the following states of each species were used: $B_{3u}, M_s = \frac{1}{2}$ for B, F and Cl; $B_{2g}, M_s = 1$ for C, O, Si and S; $B_1, M_s = \frac{1}{2}$ for OH, NO and CN and $B_{2u}, M_s = 1$ for C_2. For the initial basis set and c_{min} selection work, spin-orbit matrix element convergence used only the one-electron part of the Breit-Pauli Hamiltonian for computational ease.

A range of basis sets were chosen for each species from the Dunning set: cc-pVDZ, cc-pVTZ, cc-pVQZ and cc-pV5Z with molecular integrals obtained from both Molpro[30] and MolSOC[22,23,24]. MCCI was initially used to provide the zeroth order wavefunction for all degenerate states for each species using Slater Determinants and a single variable parameter c_{min}. For each species, the value of c_{min} was progressively lowered through the range 0.001, 0.0005, 0.0002 and 0.0001 in order to determine the effect of c_{min} on energy and spin-orbit matrix element convergence.

Once an appropriate basis set and c_{min} was selected for each species, a spin-orbit Hamiltonian matrix was then constructed in the basis of the MCCI-generated zeroth order degenerate electronic states using effective one-electron integrals. To calculate $\langle \Phi_\mu | \mathcal{H}^{so} | \Phi_\nu \rangle$, where Φ_μ and Φ_ν are the degenerate electronic states for each species, we recognise that the electronic states are constructed from a linear combination of electron configurations (Slater Determinants in this work), Ψ_a as shown in equation 9.

$$|\Phi_\mu\rangle = \sum_a^{Cfgs} c_a \, |\Psi_a\rangle \tag{9}$$

Here the c_a coefficients are determined by MCCI during calculation of the zeroth-order wavefunctions prior to calculating the spin-orbit coupling effects.

We can then write

$$\langle \Phi_\mu | \mathcal{H}^{so} | \Phi_\nu \rangle = \sum_a^{Cfgs} \sum_b^{Cfgs} c_a^* c_b \sum_{k=x,y,z} \langle \Psi_a | \mathcal{H}_k^{so} | \Psi_b \rangle \,. \tag{10}$$

These Slater Determinants are constructed from antisymmetrised permutations of the molecular orbitals, χ_i as shown in equation 11.

$$|\Psi_a\rangle = \frac{1}{\sqrt{N!}} \sum_{n=1}^{N!} (-1)^{q_n} P_n \, |\chi_i \chi_j .... \chi_k\rangle \tag{11}$$

As we only consider one-electron operators then $\langle \Psi_a | \mathcal{H}_k^{so} | \Psi_b \rangle = 0$ if there are two or more differences in their spin-orbitals while if there are no differences then the spatial symmetry of the spin-orbit operators for x, y and z means that again the contribution is zero for the systems we consider. We therefore only need to calculate the contribution in Eq. 10 when the determinants Ψ_a and Ψ_b have one difference due to spin orbitals χ_i and χ_j. If we consider the spatial $\phi(\vec{r})$ and spin $\sigma(\omega)$ components of the spin orbitals then we can factor the Breit-Pauli operator to give

$$\langle \Psi_a | \mathcal{H}_k^{so} | \Psi_b \rangle = \langle \phi_i | \mathcal{H}_{L_k}^{so} | \phi_j \rangle \, \langle \sigma_i | \mathcal{H}_{S_k}^{so} | \sigma_j \rangle \,. \tag{12}$$

Here $\mathcal{H}_{L_k}^{so}$, where $k = x, y$ or z, is the angular momentum part of the SO operator, described in equation 13 and $\mathcal{H}_{S_k}^{so}$ is the spin part, described in equation 14

$$\mathcal{H}_{L_k}^{so} = -\sum_{A=1}^{Nuc} Z_{eff}(A) \frac{[\hat{r}_{1A} \times \hat{p}(1)]_k}{r_{1A}^3}, \tag{13}$$

$$\mathcal{H}_{S_k}^{so} = -\frac{1}{2c^2} \hat{s}_k. \tag{14}$$

Integrals using the operator shown in equation 13 in the basis of molecular orbitals are provided by Molpro and MolSOC as described earlier.

The subsequent spin-orbit Hamiltonian matrix is then constructed and diagonalised to reveal the eigenvalues representing the effect of spin-orbit coupling on the splitting of the degenerate states.

Species	cc-pVDZ	cc-pVTZ	cc-pVQZ	cc-pV5Z
B	-24.590538	-24.604945	-24.621303	-24.625622
C	-37.761776	-37.788666	-37.809000	-37.813126
O	-74.910963	-74.980179	-75.013447	-75.016448
F	-99.527814	-99.624816	-99.666548	-99.667779
Si	-288.919929	-288.979740	-288.967758	-288.967758
S	-397.604530	-397.672403	-397.700078	-397.787738
Cl	-459.601919	-459.684551	-459.722033	-459.792896
OH	-75.557035	-75.632816	-75.639866	-75.641675
CN	-92.436828	-92.502282	-92.523884	-92.496162
NO	-129.578429	-129.673837	-129.678870	-129.670030
C_2	-75.718204	-75.770102	-75.774832	-75.772158

Table 1: Absolute energy convergence with basis set. MCCI c_{min} value of 0.0005. All values in Hartrees

RESULTS AND DISCUSSION

Absolute energy and spin-orbit matrix element convergence results are detailed in tables 1, 2, 3 and 4.

From tables 1 and 2, rapid convergence of both absolute energy and spin-orbit matrix element is observed at the cc-pVQZ level of basis set for B, C, O, F, Si, OH, CN, NO and C_2. It would appear that this level of basis set would be a reasonable compromise between the improved accuracy of a higher basis set and computational expense: use of the cc-pV5Z basis set appears to give only relatively small improvements in the absolute energy and spin-orbit matrix element. Difficulties are observed with CN and NO, where the absolute energy rises for the cc-pV5Z basis set. As the basis set is improved, more configurations become important and are added to the wavefunction. The wavefunction coefficients are normalised and therefore the relative importance of those configurations already in the wavefunction must drop as a result of these new configurations. Without an appropriate reduction in c_{min} to cater for this larger basis set, important configurations can be removed from the

Species	cc-pVDZ	cc-pVTZ	cc-pVQZ	cc-pV5Z
B	-9.91	-10.48	-10.71	-10.79
C	+26.47	+29.97	+28.54	+28.82
O	-101.99	-107.70	-109.77	-110.44
F	-182.09	-191.16	-194.26	-195.30
Si	+82.72	+90.63	+85.82	+85.82
S	-213.14	-224.34	-223.76	-242.42
Cl	-326.49	-338.28	-339.36	-354.15
OH	-99.28	-104.59	-106.15	-106.20
CN	-42.95	-45.59	-46.01	-46.36
NO	+91.76	+95.32	+94.91	+94.11
C_2	-25.47	-26.96	-27.39	-27.36

Table 2: Spin-orbit matrix element convergence with basis set. MCCI c_{min} value of 0.0005. All values in cm^{-1}. Only one-electron part of Breit-Pauli Hamiltonian used

Species	0.001	0.0005	0.0002	0.0001
B	-24.619254	-24.621303	-24.622837	-24.623259
C	-37.805137	-37.809000	-37.810697	-37.811156
O	-75.001373	-75.013447	-75.018209	-75.019908
F	-99.632198	-99.666548	-99.672987	-99.676072
Si	-288.960789	-288.967758	-288.973479	-288.976931
S	-397.681011	-397.700078	-397.711819	-397.716402
Cl	-459.702696	-459.722033	-459.734791	-459.741032
OH	-75.616577	-75.639866	-75.673309	-75.680552
CN	-92.476416	-92.523884	-92.560419	-92.573539
NO	-129.623605	-129.678870	-129.749042	-129.766732
C_2	-75.740761	-75.774832	-75.815557	-75.824136

Table 3: Effect of c_{min} on absolute energies. cc-pVQZ basis set used. All values in Hartrees

Species	0.001	0.0005	0.0002	0.0001
B	-10.57	-10.71	-10.71	-10.71
C	+28.50	+28.54	+28.50	+28.47
O	-109.89	-109.77	-109.44	-109.25
F	-193.88	-194.26	-194.09	-193.09
Si	+87.91	+85.82	+85.84	+85.82
S	-222.81	-223.76	-223.81	-222.69
Cl	-335.84	-339.36	-339.33	-338.77
OH	-103.97	-106.15	-105.82	-105.57
CN	-45.61	-46.01	-46.35	-46.28
NO	+93.86	+94.91	+95.77	+96.78
C_2	-27.18	-27.39	-27.41	-27.45

Table 4: Effect of c_{min} on spin-orbit matrix elements. cc-pVQZ basis set used. All values in cm^{-1}. Only one-electron part of Breit-Pauli Hamiltonian used

wavefunction during the subsequent *pruning* process, causing the absolute energy to increase. This is illustrated starkly in table 3 where reducing the c_{min} value for the CN molecule from 0.0005 to 0.0001 for the cc-pVQZ basis set causes a reduction in absolute energy from -92.560419 to -92.573539 hartrees. When the same c_{min} reduction process is applied to the cc-pV5Z basis set for both CN and NO, the problem of increasing absolute energy is resolved. It can be seen that this problem also affects C_2 although to a considerably smaller extent. This illustrates the importance of the correct choice of both basis set and c_{min} when selecting an appropriate system for calculations using MCCI. Although in all cases in table 3 show a reduction in absolute energy as c_{min} is reduced for the cc-pVQZ basis set, it is not absolute energy which is the most important characteristic. Rather, it is the spin-orbit coupling matrix element convergence which needs to be considered. Table 2 shows that the spin-orbit matrix values appear relatively invariant to the choice of basis set beyond cc-pVQZ and table 4 shows that once the cc-pVQZ basis set is chosen, the spin-orbit matrix element value is largely invariant to the c_{min} value beyond 0.0005. The exceptions are the S and Cl atoms where neither energy nor spin-orbit matrix element convergence is achieved with any basis

set.

The use of the cc-pVQZ basis set with c_{min} value of 0.0005 was therefore considered a reasonable choice overall. The exceptions are now detailed. For triplet species, all nine degenerate states must have equivalent MCCI absolute energy values. For the $M_s = 0$ values, this was found not to be the case with these states higher in energy than the others. The reason for this is straightforward. A higher number of electron configurations is required for these states than for M_s = -1,+1. To include them, a reduction in the c_{min} level is required. For C and O species the use of c_{min} = 0.0001 for the cc-pVQZ basis set for all degenerate states was sufficient to result in equivalent energies for all states as necessary for correct calculations. For Si, S and C_2, it was not computationally feasible to reduce the c_{min} value to a level which would remove this problem using the cc-pVQZ basis set. For this reason, a reduction in basis set was required. Full energy equivalence for the degenerate states was achieved for these species at the cc-pVDZ basis set using c_{min} = 0.0001. Because we wish ideally to use the smallest basis set possible in order to apply the technique to larger systems, we used the cc-pVDZ basis set and c_{min} value of 0.0001 for the other diatomic species. Although reducing the basis set below that desired results in inaccuracies in the calculations, the spin-orbit matrix elements are affected less than the absolute energies and it was considered that qualitatively, and in some cases quantitatively, these results would be reasonable. The final basis set and MCCI cut-off, c_{min} selections, along with corresponding MCCI absolute energies, for each species, are detailed in table 5. Note that a comparison with the FCI absolute energy is provided where available. Clearly MCCI, demonstrates the ability to capture much of the correlation energy of each species where data is available.

Following the determination of appropriate basis set and c_{min} value for each species, the construction of the H^{so} matrix, is performed in the basis of degenerate electronic states with matrix elements constructed as shown in equations 10, 11 and 12, using the effective one-electron Hamiltonian shown in equation 8.

The eigenvalues of the H^{so} matrix reveal the energy level shift of each of the degenerate states, allowing the multiplet width, W, and the spin orbit coupling constant, ζ, to be calculated. For doublet atomic species, the multiplet width and magnitude of spin orbit coupling constant are calculated as shown in equations 15 and 16. For triplet atomic species

Species	Basis Set	c_{min}	MCCI Absolute Energy	FCI[a] Absolute Energy	%FCI Correlation Energy
B	cc-pVQZ	0.0005	-24.621303	-24.623941	98.93%
C	cc-pVQZ	0.0001	-37.811156	-37.812622	99.99%
O	cc-pVQZ	0.0001	-75.019908		
F	cc-pVQZ	0.0005	-99.666548		
Si	cc-pVDZ	0.0001	-288.920430	-288.920678	99.99%
S	cc-pVDZ	0.0001	-397.605913	-397.606439	99.99%
Cl	cc-pVQZ	0.0005	-459.722033		
OH	cc-pVDZ	0.0001	-75.560687	-75.561567	99.99%
CN	cc-pVDZ	0.0001	-92.449939		
NO	cc-pVDZ	0.0001	-129.593930		
C_2	cc-pVDZ	0.0001	-75.727735		

Table 5: Choice of basis set and c_{min} value for each species. Comparison of MCCI absolute energy calculations with the FCI result is provided where available including the percentage of the FCI correlation energy captured by MCCI. [a]FCI values calculated as part of this work. All absolute energy values in Hartrees.

equations 17 and 18 are used. Finally, for diatomic molecules, the magnitude of the spin orbit coupling constant is the same as the multiplet width shown in the relevant equation 15 or 17 depending on the spin of the species. For these equations, E_J is the energy of the level of total angular momentum J, and the Lande interval rule is employed.

$$W = |E_{3/2} - E_{1/2}| \tag{15}$$

$$|\zeta| = \frac{2}{3}W \tag{16}$$

$$W = |E_2 - E_0| \tag{17}$$

$$|\zeta| = \frac{1}{3}W \tag{18}$$

Table 6, details the relative numbers of electron configurations required using MCCI compared to those required for an FCI solution. From the tables therefore, it can be seen that, for all systems, MCCI achieves good agreement with experiment using just a fraction of the available FCI space. The calculated results are, on the whole, in good enough agreement with experiment to suggest that MCCI could be used as an alternative method for investigating spin-orbit coupling effects with the method's inherent advantage of the formation of highly compact wavefunctions and the ability to perform an essentially black-box treatment of the system where prior knowledge of the important orbitals is not required.

Having proved the applicability of the technique to these test-bed systems, we now briefly present application of this method to predict the spin-orbit interactions between the $X^3\Sigma_g^-$ and both the $a^1\Delta_g$ and $b^1\Sigma_g^+$ states of the O_2 molecule, a more detailed discussion of which can be found in the literature.[47] Transitions between the triplet ground state and the two lowest energy singlet states of molecular oxygen are formally forbidden on the grounds of both spatial and spin symmetry. In reality, both transitions are observed experimentally. The $a^1\Delta_g$ state lies at 7918.1 cm^{-1} above the triplet ground state with the $b^1\Sigma_g^+$ lying at 13195.1 cm^{-1} above the triplet[44]. Spin-orbit coupling drives the dynamics behind these "forbidden" transitions through mixing of the singlets and the $M_S = 0$ of the triplet. This is

System	**Basis**	c_{min}	**FCI**[a] **Fraction**	ζ_{MCCI} [b]	$\zeta_{exp.}$ [c]	W_{MCCI} [d]	$W_{exp.}$ [e]
B	cc-pVQZ	0.0005	3 x 10^{-5}	+9.41	+10.19	14.12	15.29
C	cc-pVQZ	0.0001	1 x 10^{-5}	+14.29	+14.47	42.86	43.41
O	cc-pVQZ	0.0001	1 x 10^{-7}	-68.71	-75.66	206.12	226.98
F	cc-pVQZ	0.0005	3 x 10^{-9}	-269.01	-269.39	403.51	404.14
Si	cc-pVDZ	0.0001	2 x 10^{-6}	+64.31	+74.39	192.94	223.16
S	cc-pVDZ	0.0001	2.0 10^{-6}	-172.46	-191.21	517.37	573.64
Cl	cc-pVQZ	0.0005	2 x 10^{-16}	-553.28	-588.23	829.93	882.34
OH	cc-pVDZ	0.0001	2 x 10^{-4}	-124.78	-139.21	124.78	139.21
C_2	cc-pVDZ	0.0001	4 x 10^{-7}	-25.40	-15.25	25.40	15.25
CN	cc-pVDZ	0.0001	1 x 10^{-7}	-47.09	-52.64	47.09	52.64
NO	cc-pVDZ	0.0001	2 x 10^{-8}	+110.30	+123.16	110.30	123.16

Table 6: Calculated results for all species in this work. Slater Determinants are used in all cases. [a]This is the fraction of electron configurations from FCI space which MCCI has recovered. [b]Spin-orbit coupling constant as calculated by MCCI in this work. Units cm^{-1}. [c]Experimental spin-orbit coupling constant. Units cm^{-1}. [d]Multiplet width as calculated by MCCI in this work. Units cm^{-1}. [e]Experimental multiplet width. Units cm^{-1}.

understood by analysis of the effect of the spin-orbit coupling first-order perturbation on the wavefunctions as shown in equation 19 where the left hand side is the first-order perturbed (due to spin-orbit coupling) wavefunction of the state. Ψ_i is the unperturbed wavefunction of state i and Ψ_j is the state which couples with Ψ_i.

The probability of a transition from the triplet state to the $b^1\Sigma_g^+$ is considerably larger than of the transition from the triplet to the $a^1\Delta_g$ state. As expected, we find that the spin-orbit coupling interaction between the triplet and $b^1\Sigma_g^+$ states is correspondingly much larger than between the triplet and the $a^1\Delta_g$ state. Semi-empirical calculations predict a spin-orbit coupling matrix element magnitude of 153 cm^{-1} for the interaction between the triplet and the $b^1\Sigma_g^+$ state with subsequent *ab-initio* calculations[47] finding this value to be closer to 176 cm^{-1}. Using MCCI, our calculations predict the magnitude of this spin-orbit matrix element to be 160 cm^{-1} - in good agreement.

Substituting the relevant calculated values into equation 19 shows mixing of the triplet and $b^1\Sigma_g^+$ state with the perturbed triplet wavefunction found to comprise 98.8% triplet and 1.2% singlet. Our calculations also predict a spin-orbit matrix element magnitude of 2.99 cm^{-1} between the triplet state and the $a^1\Delta_g$ state. This is considerably smaller than that of the triplet to $b^1\Sigma_g^+$ state interaction and therefore is, qualitatively at least, in line with expectations. The mixing between triplet and $a^1\Delta_g$ states shows that this singlet contributes around 0.036% to the perturbed triplet wavefunction, which is suggestive of a subsequent reduction in transition intensity. This explains the weakened interaction and the lower probability of a transition between these states. Finally, our calculations predict the magnitude of the spin-orbit matrix element between the $a^1\Delta_g$ and $b^1\Sigma_g^+$ states to be 2.39 cm^{-1}. This transition is known to have a low probability and again the calculated spin orbit matrix element would appear to be qualitatively in line with expectations. Our calculations predict that the mixing between the singlet states is negligible with both perturbed wavefunctions consisting of only about 0.044% contribution from the other.

$$\widetilde{\Phi}_i = \Phi_i + \sum_{j \neq i} \frac{\langle \Phi_i | H^{SO} | \Phi_j \rangle}{E_i - E_j} \Phi_j \tag{19}$$

We now explore the applicability of MCCI to more multi-reference systems in order to

further explore the advantages both of the highly compact wavefunctions of MCCI and the black box nature of the method. In order to do this, we present a brief discussion of the OH radical with stretched bond length of 2.5 Å, and first compare MCCI results of spin orbit coupling constants with the FCI value when using the 3-21G basis and effective one-electron integrals for both. The multi-reference nature of this system can be estimated from the MCCI wavefunction using equation 20, where c_i is the coefficient of the $i-$th electronic configuration in the wavefunction and the summation is over all configurations in the wavefunction.

$$MR = \sum_i |c_i|^2 - |c_i|^4 \tag{20}$$

This equation gives a result between *0* and *1*, where a value of *0* indicates a single reference wavefunction and a value of *1* indicates a highly multi-reference system. For the OH radical stretched to 2.5 Å, the 3-21G FCI calculation gives $MR = 0.66$ demonstrating the multireference character in this case.

We see in Fig. 1 that the MCCI spin-orbit coupling constant has essentially converged to the FCI result on the scale of the graph when the cutoff is lowered to 10^{-4}. This used only 1572 Slater determinants on average compared with 38136 for the FCI wavefunction and so represents around 4% of the FCI space of this multireference system when using a small basis. The inset of Fig. 1 shows that the spin-orbit coupling constant is much more sensitive to the quality of the wavefunction than the correlation energy. Even with a cutoff of 5×10^{-3}, giving a MCCI wavefunction of 97 Slater determinants on average, most of the -0.262 Hartree correlation energy is recovered but the spin-orbit coupling constant has almost 40% error and we have to reduce the cutoff to 10^{-4} to get accurate results for both quantities.

We next consider a larger basis set (cc-pVDZ) and a cutoff of 10^{-4}. We find that for MR a value of 0.68 is obtained (compared to a value of 0.10 at equilibrium bond length) Clearly then, we see the onset of a more multi-reference description for this stretched system when using cc-pVDZ. We now compare MCCI results of spin orbit coupling constants and number of necessary electronic configurations in the resulting wavefunction with those obtained using MRCI in Molpro[30] for a variety of active spaces.

Results are shown in table 7, with all results obtained using cc-pVDZ basis set. MCCI

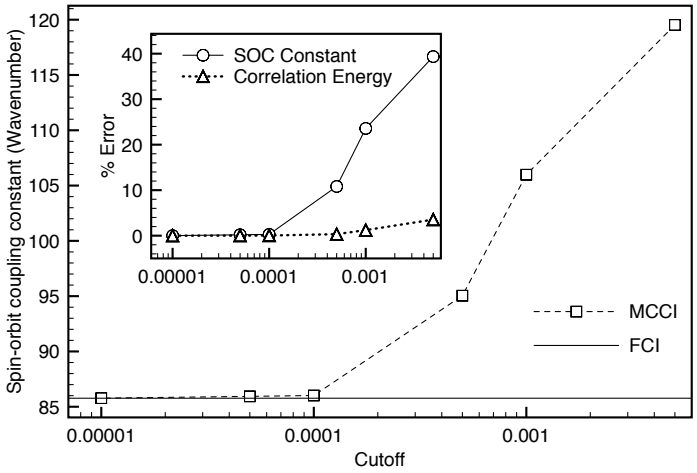

Figure 1: Spin-orbit coupling constant (cm^{-1}) for stretched OH ($R = 2.5$Å) with a 3-21G basis plotted against MCCI cutoff (c_{min}) on a logarithmic scale. Inset: Percentage error of the MCCI spin-orbit coupling constant and correlation energy when compared with the FCI result versus MCCI cutoff (c_{min}) on a logarithmic scale.

results were obtained using c_{min} of 0.0001.

From these results, it is clear that the choice of active space is crucial in obtaining a good solution using MRCI. A range for the spin-orbit coupling constant of more than 30 cm^{-1} is found for the selection of active spaces shown. The choice of active space is therefore crucial in obtaining even qualitative results if comparison is made with the FCI result of -99.79 cm^{-1}. The FCI result uses the full Breit-Pauli operator while the MRCI values use this for the

Method	Active Space	ζ	**Configs**
HF	-	-138.56	1
MCCI	-	-104.01	8388 SDs
MRCI	$2a_1 3a_1 1b_1 2b_1 1b_2 2b_2$	-131.02	9994 CSFs
MRCI	$1a_1 2a_1 3a_1 1b_1 2b_1 1b_2 2b_2$	-122.11	36830 CSFs
MRCI	$1a_1 2a_1 3a_1 4a_1 1b_1 2b_1 1b_2 2b_2$	-99.53	99600 CSFs
MRCI	$1a_1 2a_1 3a_1 4a_1 1b_1 2b_1 3b_1 1b_2 2b_2 3b_2$	-99.42	448662 CSFs
MRCI	$1a_1 2a_1 3a_1 4a_1 5a_1 1b_1 2b_1 3b_1 1b_2 2b_2 3b_2 1a_2$	-99.70	1279092 CSFs
FCI	-	-99.79	11267456 SDs

Table 7: Comparison of stretched OH radical (bond length 2.5 Å) spin-orbit coupling constants and numbers of electronic configurations between MCCI and MRCI for a range of active spaces. cc-pVDZ basis set used throughout. MCCI results use c_{min} of 0.0001. MCCI energy convergence is 0.001 Hartrees. ζ values in cm^{-1}. MCCI number of configurations is the average number of Slater determinants (SDs) across the four degenerate state calculations while uncontracted configuration state functions (CSFs) are reported for MRCI and FCI. The FCI result uses the full Breit-Pauli operator while the MRCI values use this for the internal configurations and a mean-field one-electron fock operator for the external configurations.

internal configurations otherwise a mean-field one-electron fock operator is employed. MCCI is able to achieve results within 4.23% of the FCI spin-orbit coupling constant result using just 8388 Slater determinants (around 0.074% of the FCI space) compared to a minimum of 99,600 uncontracted configuration state functions (CSFs) with MRCI. Although the number of contracted CSFs is lower at 13,004 we note that more configurations will be required to represent these as Slater determinants. In the MCCI case, the only selectable parameter is the setting of c_{min}. In this way, the two major advantages of MCCI are demonstrated: good qualitative results can be obtained using a highly compact wavefunction and no prior knowledge of important orbitals is required in order to achieve these results.

Finally, we briefly mention the repeatability of our results. For any stochastic technique, it can be expected that running the calculations repeatedly will give different results. We therefore tested the standard deviation of the results using the ^2P state of the boron atom over 10 runs with basis set cc-pVQZ and c_{min} of 0.0001 and energy convergence of 0.001 Hartrees. The standard deviation of our results was 0.005 cm^{-1}. This gives an indication of the high reliability of our calculations.

The majority of the observed errors in our calculations when compared to experiment are thought to be down to a combination of the size of the basis set, errors using the effective one-electron approximation and the failure to capture all relevant electron configurations in the wavefunction. These results however are good enough to suggest that MCCI may well be a useful tool for calculating quantities such as approximate singlet-triplet interactions in addition to splitting of degenerate energy levels where absolute accuracy in the results is less important than a good qualitative picture. The loss in accuracy in these results is very small in spite of our use of small basis sets. The main advantage of MCCI is that such good results can be obtained using more compact wavefunctions without prior knowledge of the important orbitals and this might lead the technique to be useful for larger multi-reference molecules where other techniques may be too computationally expensive.

CONCLUSIONS

MCCI has shown promise as a technique for calculating spin-orbit coupling properties using highly compact wavefunctions without prior knowledge of the important orbitals. Good agreement with experiment is shown in this first proof-of-concept work for atomic species and this is extended through to the diatomic species despite the use of the relatively small cc-pVDZ basis set. The key objective in our use of MCCI is not to demonstrate a more accurate method for calculating spin-orbit properties than other techniques but to illustrate the potential for using this technique on larger multi-reference systems, taking advantage of the highly compact wavefunctions and the subsequent good results obtained using small basis sets without prior knowledge of the important orbitals. In this regard, it is clear that the method performs well in predicting singlet-triplet interactions between the $X^3\Sigma_g^-$ and the $b^1\Sigma_g^+$ states of the O_2 molecule. Of course, other techniques such as CASSCF and MRCI are commonly used in such molecules, producing more accurate results than MCCI but both techniques require prior knowledge of the important orbitals of the system. For example, MRCI predictions for the spin-orbit matrix elements for species such as the ^2P state of the Cl atom are shown to vary by as much as 28 cm^{-1} depending on the choice of active space[13]. Our own findings add to this, finding a variation of around 32 cm^{-1} on the MRCI values of spin-orbit coupling constant predicted for the stretched OH radical depending on the chosen active space. MCCI does not require prior knowledge of the active space and hence allows an essentially black box treatment of the molecule with only a single controllable parameter c_{min} needed. There are however disadvantages in this approach. CASSCF and MRCI calculations partition the resulting orbital space. This partitioning has the potential to ease further calculations on the orbitals as it may, for instance, be possible to identify integrals or derivatives which may be zero in subsequent property calculations without having to explicitly make those calculations. MCCI does not partition the orbital space and so is unable to take advantage of these simplifications - all derivatives for example would have to be explicitly calculated. Therefore, like all techniques, MCCI has advantages and disadvantages and these must be weighed up when using the method.

It is our intention to follow up this initial proof-of-concept work with a more detailed

analysis of the applicability of the technique to a wide range of multi-reference systems.

ACKNOWLEDGMENTS

MJP and JPC thank the Leverhulme Trust for funding (RPG-2015-215); MJP also thanks the EPSRC for funding through the platform grant EP/P001459/1; PM thanks the EPRSC for support through a DTP studentship.

References

1. Chambaud, G., Gritli, H., Rosmus, P., Werner, H. -J., Knowles, P. J., Mol. Phys., **2000**, 98, 1793-1802.

2. Furlani, T.R., King, H.F., J. Chem. Phys., **1985**, 82, 12, 5577-5583.

3. Beljonne, D., Shuai, Z., Pourtois, G., Bredas, J.L., J. Phys. Chem. A, **2001**, 105, 3899-3907.

4. Li, R., Wei, C., Sun, Q., Sun, E., Xu, H., Yan, B., J. Phys. Chem. A, **2013**, 117, 2373-2382.

5. Li, R., Zhang, X., Feng, W., Jiang, Y., Fei, D., Jin, M., Yan, B., Xu, H., Comp. Theor. Chem., **2014**, 1032, 20-26.

6. Li, R., Wei, C., Sun, Q., Sun, E., Jin, M., Xu, H., Yan, B., J. Quant. Spec. Rad. Trans., **2014**, 133, 271-280.

7. Blume, M., Watson, R.E., Proc. Roy. Soc. Lond. A., **1962**, 270, 1340, 127-143.

8. Blume, M., Watson, R.E., Proc. Roy. Soc. Lond. A., **1962**, 271, 1347, 565-578.

9. Walker, T.E.H., Richards, W.G., Symp. Far. Soc., **1968**, 2, 64-68.

10. Koseki, S., Schmidt, M., Gordon, M., J. Phys. Chem., **1992**, 96, 26, 10768-10772.

11. Heß, B.A., Marian, C.M., Wahlgren, U., Gropen, O., Chem. Phys. Lett., **1996**, 251, 365-371.

12. Nicklass, A., Peterson, K.A., Berning, A., Werner, H. -J., Knowles, P. J., J. Chem. Phys., **2000**, 112, 13, 5624-5632.

13. Berning, A., Schweizer, M., Werner, H. -J., Knowles, P. J., Palmieri, P., Mol. Phys., **2000**, 98, 21, 1823-1833.

14. Tu, Z., Wang, F., Li, X., J. Chem. Phys., **2012**, 136, 174102.

15. Epifanovsky, E., Klein, K., Stopkowicz, S., Gauss, J., Krylov, A.I., J. Chem. Phys., **2015**, 143, 064102.

16. Mück, L.A., Gauss, J., J. Chem. Phys., **2012**, 136, 111103.

17. Roemelt, M., Maganas, D., DeBeer, S., Neese, F., J. Chem. Phys., **2013**, 138, 204101.

18. Irmer, S., Frank, T., Putz, S., Gmitra, M., Kochan, D., Fabian, J., Phys. Rev. B, **2015**, 91, 115141.

19. Maganas, D., Roemelt, M., Hävecker, M., Trunschke, A., Knop-Gericke, A., Schlögl, R., Neese, F., Phys. Chem. Chem. Phys., **2013**, 15, 7260-7276.

20. Kim, I., Park, Y.C., Kim, H., Lee, Y.S., Chem. Phys., **2012**, 395, 115-121.

21. Liu, H., Shi, D., Sun, J., Zhu, Z., J. Quant. Spec. Rad. Trans., **2015**, 151, 155-168.

22. Chiodo, S. G., Russo, N., J. Comput. Chem., **2008**, 29, 912-920.

23. Chiodo, S. G., Russo, N., J. Comput. Chem., **2009**, 30, 832-839.

24. Chiodo, S. G., Leopoldini, M., Comp. Phys. Comm., **2014**, 185, 676-683.

25. Greer, J.C., J. Chem. Phys., **1995**, 103, 5, 1821-1828.

26. Greer, J.C., J. Comp. Phys., **1998**, 146, 181-202.

27. Tong, L., Nolan, M., Cheng, T., Greer, J.C., Comp. Phys. Comm., **2000**, 131, 142-163.

28. Coe, J. P., Paterson, M. J., Rec. Res. Dev. Chem. Phys., **2012**, 6, 41-65.

29. Coe, J. P., Paterson, M. J., Int. J. Quant. Chem., **2016**, 116, 1772-1782.

30. Werner, H.-J., Knowles, P. J., Knizia, G., Manby, F.R., Schütz, M., *et al.*, Molpro version 2015.1, a package of *ab initio* programs, see http://www.molpro.net, **2015**.

31. Lischka, H., Shepard, R., Shavitt, I., Pitzer, R.M., Dallos, M., Müller, T., *et al.*, Columbus, An *ab initio* Electronic Structure Program, Release 5.9,2, available at http://www.univie.ac.at/columbus, **2008**.

32. Coe, J. P., Paterson, M. J., J. Chem. Phys., **2012**, 137, 204108.

33. Győrffy, W., Bartlett, R.J., Greer, J.C., J. Chem. Phys., **2008**, 129, 064103.

34. Coe, J. P., Taylor, D.J., Paterson, M. J., J. Chem. Phys., **2012**, 137, 194111.

35. Coe, J. P., Taylor, D.J., Paterson, M. J., J. Comp. Phys., **2013**, 34, 1083-1093.

36. Booth, G, H., Thom, A. J. W., Alavi, A., J. Chem. Phys., **2009**, 131, 054106.

37. Coe, J. P., Paterson, M. J., Chem. Phys., **2013**, 139, 154103.

38. Coe, J. P., Paterson, M. J., J. Chem. Phys., **2014**, 141, 12, 124118.

39. Coe, J. P., Paterson, M. J., Theor. Chem. Acc., **2015**, 134, 58.

40. Coe, J. P., Paterson, M. J., Chem. Phys. Lett., **2016**, 645, 106-111.

41. Coe, J. P., Murphy, P., Paterson, M. J., Chem. Phys. Lett., **2014**, 604, 46-52.

42. Knowles, P. J., Handy, N. C., Chem. Phys. Lett., **1989**, 111, 4-5, 315-321.

43. Knowles, P. J., Handy, N. C., Comp. Phys. Comm., **1989**, 54, 75-83.

44. Huber, K. P., Herzberg, G., in NIST Chemistry WebBook, NIST Standard Reference Database Number 69, Eds. P.J. Linstrom and W.G. Mallard, National Institute of Standards and Technology, Gaithersburg MD, 20899, doi:10.18434/T4D303, (retrieved April 26, 2017)

45. Cooper, D. L., Wilson, S., J. Phys. B: At. Mol. Phys., **1982**, 15, 493-501.

46. Cooper, D. L., Wilson, S., J. Chem. Phys., **1982**, 76, 12, 6088-6090.

47. Minaev, B., Vahtras, O., Ågren, H., Chem. Phys., **1996**, 208, 299-311.